Macromolecular Rapid Communications
www.mrc-journal.de

Adaptation and Recovery of a Styrene-Acrylic Acid Copolymer Surface to Water

Xiaomei Li, Mirela Encheva, Hans-Jürgen Butt, Ellen H. G. Backus, and Rüdiger Berger**

Drops sliding down an adaptive surface lead to changes of the dynamic contact angles. Two adaptation processes play a role: 1) the adaptation of the surface upon bringing it into contact to the drop (wetting) and 2) the adaptation of the surface after the drop passed (dewetting). In order to study both processes, the authors investigate samples made from random styrene (PS)/acrylic acid (PAA) copolymers, which are exposed to water. Sum-frequency generation spectroscopy and tilted-plate measurements indicate that during wetting, the PS segments displace from the interface, while PAA segments are enriched. This structural adaptation of the PS/PAA random copolymer to water remains after dewetting. Annealing the adapted polymer induces reorientation of the PS segments to the surface.

1. Introduction

Surfaces can change their chemical-physical properties when coming into contact with liquids. The umbrella term for those processes is surface adaptation.[1,2] Adaptation processes can be reversible, like swelling of polymers by diffusion of molecules.[3–5] Mixing of two polymers may result in selective swelling of one of them. In some cases, the swelling process leads to a preferential enrichment of the more compatible component to the selected liquid.[6–10] Then the adaptation process may become nonreversible. Both, reversible and nonreversible adaptation processes provide potential to create smart surfaces for sensors[11] and biomedical applications.[12]

When a drop is sliding over an adaptive surface, two phenomena play a role: 1) the adaptation of the surface upon bringing it in contact with the liquid on the advancing side of the drop (wetting process) and 2) the adaptation of the surface after the drop passed (dewetting process). In this context, measuring drop velocity-dependent dynamic contact angles is an elegant way to understand the wetting and dewetting kinetics. In a previous study,[13] we investigated the wetting process by measuring velocity dependent dynamic contact angles on a random copolymer composed of styrene and 11–25 mol% acrylic acid (PS/PAA). Both, the advancing and the receding contact angles decreased when thePS/PAA surface adapted to water. This adaptation could occur due to water diffusion into the polymer layer and/or PAA enrichment at the surface (**Figure 1**). We have verified the presence of water diffusion by fluorescence microscopy measurement, but we had no direct proof of water induced PAA enrichment at the interface. Here, we address the questions: Does the copolymer surfaces enrich with one component of the PS/PAA upon wetting with water? Is such an enrichment permanent after dewetting? Does the enrichment change with the number of sliding water drops?

2. Results and Discussions

2.1. Sum-Frequency Generation Spectroscopy (SFG)

In order to probe the adaptation and recovery of the PS/PAA copolymer surface, we used sum-frequency generation spectroscopy (SFG). SFG is a technique that provides a vibrational spectrum of interfacial molecules. In SFG an infrared (IR-ω_{IR}) and a visible (VIS-ω_{VIS}) laser pulse are overlapped in space and time to generate a third beam (SF), the frequency of which results from the addition of the previous two ($\omega_{SFG} = \omega_{IR} + \omega_{VIS}$). This third beam (SF) can only be produced in noncentrosymmetric environments, making SFG stand out as a powerful tool for analyzing interfaces (**Figure 2**A).[14] If the IR-beam is in resonance with the vibrational modes of the surface molecules, the SFG signal will be enhanced producing a vibrational spectrum of the interfacial molecules.[14] The intensity of the resulting spectrum is proportional not only to the density of the molecular groups but also to their orientation, leading to higher intensity values for ordered systems than for randomly organized ones.

In order to perform SFG experiments, the PS/PAA copolymer was spin-coated on CaF_2 windows. Before the SFG measurements, the resulting layers were annealed in an oven at 150 °C for 60 min. In order to determine a restructuring of the PS/PAA copolymer, vibrational spectra were acquired before and after wetting the sample. To assure that the spectra obtained before and

X. Li, H.-J. Butt, R. Berger
Max Planck Institute for Polymer Research
Ackermannweg 10, Mainz 55128, Germany
E-mail: berger@mpip-mainz.mpg.de
M. Encheva, E. H. G. Backus
Department of Physical Chemistry
University of Vienna
Währinger Straße 42, Vienna 1090, Austria
E-mail: ellen.backus@univie.ac.at
The ORCID identification number(s) for the author(s) of this article can be found under https://doi.org/10.1002/marc.202100733

DOI: 10.1002/marc.202100733

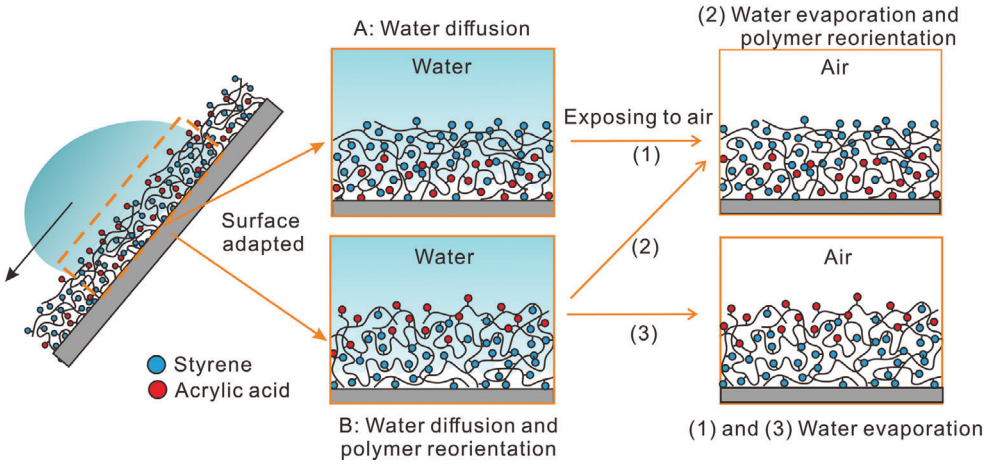

Figure 1. A,B) Possible adaptation and 1–3) recovery processes of a PS/PAA copolymer surface upon wetting.

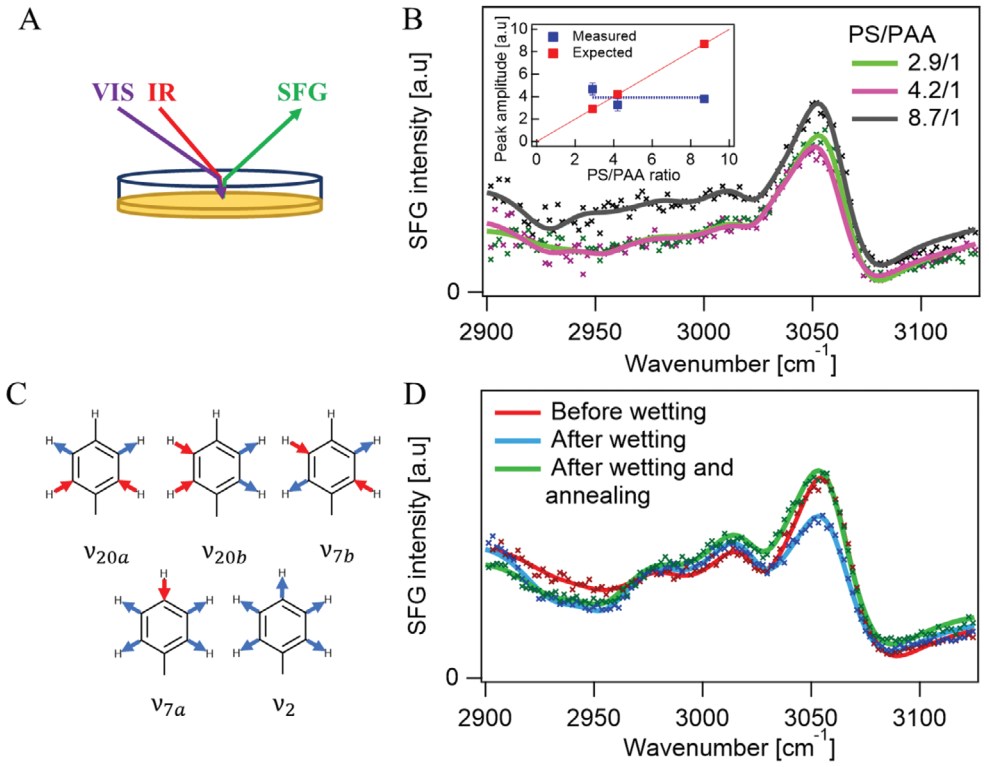

Figure 2. A) Working principle of sum frequency generation; B) SFG spectra of different PS/PAA ratios after annealing and their correspondent fits. The inset shows the measured and expected (based on PS fraction) peak amplitude as function of PS/PAA ratio; C) Phenyl ring C–H stretching vibrational modes; D) SFG spectrum of 130 nm 8.7/1 PS/PAA in SSP polarization before contact with water (red), after (blue) contact with water, and after annealing again (green) with their corresponding fit.

after wetting were measured on exactly the same spot at the interface, the surface was wetted using a flow cell. The IR and VIS beams transmit through the CaF_2 window before hitting the polymer layer (Figure 2A). Our sample entails the CaF_2–PS/PAA and the PS/PAA–air interface, both of which can contribute to the SFG-signal. We are interested in the PS/PAA–air interface, since it is the one that can be directly exposed to water. Therefore, we have adjusted the PS/PAA film thickness in order to obtain an SFG-signal dominated by the PS/PAA–air interface (Sections SI1 and SI2, Supporting Information).[15]

Figure 2B shows SFG spectra of spin coated and annealed films made from polymers that have different ratios of PS/PAA: 8.7/1, 4.2/1, and 2.9/1. All three spectra show a dominating signal at ~3060 cm^{-1}. To quantify the signal intensity, we fit the SFG data with a sum of Lorentzian line-shapes representing each resonance.[16] A minimum of nine Lorentzian peaks, assigned ac-

Table 1. Assignments for PS/PAA SFG spectra.

Wave number [cm^{-1}]	FWHM [cm^{-1}]	Relative sign of amplitude	Assignment
2907	100	+	CH_2 as
2931	36	−	CH_3 Fermi
2956	28	−	CH_3 as
2980	30	+	Combination mode
3016	34	+	ν_{20b}
3030	19	−	ν_{7a}
3057	40	+	ν_{7b} and ν_2
3076	55	−	ν_{20a}
3693	250	+	OH

cording to literature, are needed in order to describe the spectrum correctly (**Table 1**).[17–20] The different ring modes are schematically depicted in Figure 2C.

The assignment shows that the phenyl rings of the PS part of the copolymer produce several CH stretching vibrations (3016, 3030, 3057, and 3076 cm^{-1}). The resonances below 3000 cm^{-1} can be either from PS or from PAA. As the 3057 cm^{-1} peak is by far the most intense, we decided to use it as a marker of the PS surface contribution. The blue squares in the inset in Figure 2B show that the amplitude of the 3057 cm^{-1} band is independent of the PS/PAA ratio. In principle, one might expect that the amplitude of this band scales linear with the amount of PS in the layer schematically represented by the red data-points in the inset of Figure 2B. Thus, we conclude that independently of the PS/PAA ratio indicated, the same amount of PS groups is present at the polymer–air interface after annealing.

Upon wetting with water, the surface adapts and the contact angle reduces.[13] However, it is unclear if this adaption will lead to a permanent reorientation of the PS even after drying the surface. Here we use SFG to determine the surface structure of the PS/PAA 8.7/1 sample after the wetting and dewetting process. The corresponding samples were wetted with water. After 3 min, the water was removed and the samples were dried by blowing dry air. Right after that, an SFG spectrum was acquired from the same measuring spot as the first one. Clearly, the intensity of the 3057 cm^{-1} band, used as a marker of the phenyl side chain of the PS segments, reduces upon wetting (Figure 2D, blue curve). From the spectra in the OH stretch region (see Figure S6 in Section SI3, Supporting Information), we have no indication that water remains in the surface region of the layer. Fitting the spectra reveals that the amplitude of the 3057 cm^{-1} peak decreases by 16 ± 7%. This decrease of the signal could originate from a displacement of the PS rings from the surface or from a reorientation of the rings. Experiments under different polarization combinations could provide information about orientational changes of molecular groups. As upon wetting the SSP, SPS, and PSS signal decrease, the SFG data indicate that the decrease of the signal is due to displacement of the PS rings from the surface (see Section SI1, Supporting Information). Moreover, as the signal for a pure PS film shows in contrary a small increase before and after wetting (see Figure S7 in Section SI4, Supporting Information), possibly due to a small reorientation, the observed decrease for the PS/PAA layer is assigned to a displacement of the PS rings from the surface, reducing the hydrophobicity of the resulting surface. Thus, the wetting and dewetting process of the PS/PAA sample surface results in a permanent restructuring of molecular groups on the interface. However, after annealing the sample at 150 °C for 1 h the SFG spectrum is similar to the one before wetting (Figure 2D, green curve). Therefore, we can affirm that annealing reverses the adaptation of the surface into a state very similar to the pristine sample.

The SFG results indicate that the PS segments are displaced from the interface after being exposed to water. We attribute this displacement to a movement of the PS segments away from the interface and enrichment of the PAA segments toward the surface. Unfortunately, we were unable to detect the C═O vibration of the PAA segment with SFG to support this conclusion, as we lack sensitivity to the PS/PAA–air interface for this vibration (see Figure S4 in Section SI2, Supporting Information). However, as mentioned above, the decrease in different polarizations already points to a removal of phenyl rings at the surface.

2.2. Contact angle dependence

In order to quantify the fraction of PS segments (ϕ) at the interface, we measured the advancing contact angles of PS/PAA surfaces after being wetted and annealed at temperature from 50 to 150 °C. All advancing contact angles of PS/PAA surfaces with different ratios are between 94° and 98° after annealing the samples at 150 °C (**Figure 3**A). These values are only a little bit lower than the advancing contact angle of a surface made from pure PS, θ_{PS}, which is around 100°. Therefore, the contact angle measurements are consistent with the interpretation of the SFG signals, which revealed that the amount of air-exposed PS groups is independent of the PS/PAA ratio. Surfaces of pure PAA are soluble in water and therefore hydrophilic. Due to this, we assume an advancing contact angle θ_{PAA} of 0°. According to the Cassie model,[21]

$$\cos\theta_{PS/PAA} = \varphi\cos\theta_{PS} + (1-\varphi)\ \cos\theta_{PAA} \quad (1)$$

we calculated the PS fraction at the interface of the PS/PAA surfaces with different ratios. After covering the surface with a water drop for 30 min, the advancing angle of 8.7/1 PS/PAA surfaces decreased from 99° to 88°. Correspondingly, the PS-fraction decreases from 98% to 82% at the interface, which is consistent with the decrease of the SFG intensity. After annealing the adapted PS/PAA surface at 50, 75, and 100 °C for 30 min each, the advancing contact angles increased gradually (Figure 3A). This conclusion is supported by SFG experiments performed after annealing at different temperatures showing an increasing recovery with increasing annealing temperature (see Figure S8 in Section SI5, Supporting Information). PS/PAA surfaces with ratios of 4.2/1 and 2.9/1 PS/PAA follow a similar trend with advancing angles 1–5° lower compared to 8.7/1 PS/PAA surfaces. Correspondingly, we obtain 1.5–7.5% less PS at the interface. Also for poly(α-hydroxymethyl-*n*-butylacrylate) and poly(methyl methacrylate) films, a change in the contact angle and SFG signal has been observed and assigned to a larger exposure of the hydrophilic groups to the interface.[22,23] For the butylacrylate film, annealing in water above the T_g enhances the restructuring.[22]

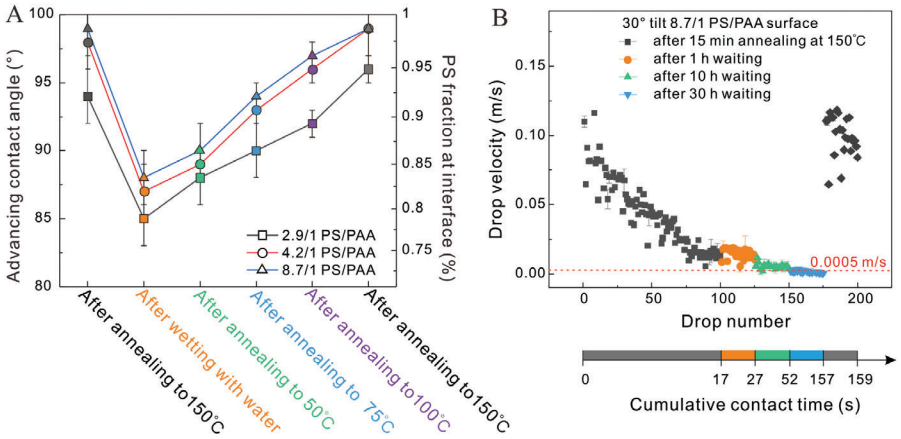

Figure 3. A) Advancing contact angles and corresponding PS fractions at the interfaces of 2.9/1, 4.2/1, and 8.7/1 PS/PAA after being covered with a water drop for 30 min and annealing at temperatures of 50, 75, 100, and 150 °C for 30 min, respectively. The errors were determined by averaging over three experiments. B) Drop velocities versus drop number. Measurements were performed at a tilt angle of 30° on an 8.7/1 PS/PAA surface with drop interval of 1 min after surface annealing at 150 °C for 15 min (drop 1–drop 100, drop 176–drop 200), waiting for 1 h (drop 101–drop 125), 10 h (drop 126–drop 150), and 30 h (drop 151–drop 175). Note: cumulative contact time = $\sum_{n} \frac{\text{Drop length}}{\text{drop velocity}}$ (n is drop number).

Subsequently, we measured how the PS/PAA copolymer surfaces adapt owing to a sliding drop. We measured the velocity of sliding drops with a drop interval of 1 min. For the first 100 drops the velocity decreased with increasing drop number (Figure 3B). Thus, the surface adapts more and more for subsequent drops. In order to test if there would be a partial recovery of the surface for longer waiting times, that is, exposure to air, we stopped the drop deposition and waited for 1 h. The velocity of the 101th drop didn't increase and subsequent drops exhibited a further slight decrease in drop velocity (Figure 3B). We even extended the waiting time to 30 h; the drop velocity remained constant (Figure 3B). Thus, at room temperature the surface does not recover. However, annealing the surface at temperature of 150 °C for 15 min, led to an increase in drop velocity to the same level of the first drop. For subsequent drops, the drop velocity decreased at a similar trend like the first 100 drops (Figure 3B). The latter indicates that the surface recovered by annealing, consistent with the SFG results (Figure S8 in Section SI5, Supporting Information) and contact angle measurements (Figure 3A and Figure S9 in Section SI6, Supporting Information). The observation that the adapted PS/PAA surface cannot recover at room temperature, but only after being annealed is attributed to the memory effect of polymers.[24–26]

3. Summar and Conclusions

In summary, annealed PS/PAA copolymer surfaces adapt nonreversibly to wetting by water. The SFG measurements indicated that the PS segments are displaced from the interface and PAA segments enrich at the surface. The latter results in the observed decrease in the advancing contact angles. Thus, adaptation of PS/PAA copolymer surfaces is given by both water diffusion into the sample (swelling)—as previously proven by fluorescence microscopy—and polymer reorientation at the surface. To which extend swelling and reconstruction contribute to the decrease in sliding velocity, respectively, is not yet clear. We exclude plastic deformation of the surface, because the surface roughness remains constant. Additionally, elastic deformation of the sample surface may happen near the three-phase contact line[27] and contribute to the decrease in sliding velocity. Both, the analysis of the SFG and contact angle measurements suggest a decrease of the PS content at the surface by about 16% after wetting with water for the 8.7/1 PS/PAA copolymer. This decrease is not considerably influenced by increasing the PAA content in the copolymer (Figure 3A). Therefore, the contact angles are still dominated by styrene and a transition to a fully PAA dominated surface does not take place. Interestingly, in the sliding drop experiment the enrichment of acrylic acid groups at the surface increases with drop number. Thus, the contact time of the surface with water corresponds to 50 ms for a drop velocity of 0.1 m s^{-1} and a drop length of 5 mm. Therefore, by controlling the contact time (e.g., using the tilt angle) and the drop number, the enrichment of acrylic acid at the surface can be controlled. A saturated state is observed after about 150 drops have passed. The accumulated contact time in this case corresponds to 157 s (Figure 3B). The time the water was kept in contact with the sample in the SFG-experiment was 180 s. Thus, the SFG measurement corresponds to the saturated state.

4. Experimental Section

Preparation of PS/PAA Copolymer Surfaces: For details, the authors referred to their previous work.[13] The characteristics of the synthesized PS/PAA random copolymer is summarized in Section S7, Supporting Information. Briefly, after synthesis, the PS/PAA random copolymer was dissolved in THF (1.5 wt%). Then the solution was spin-coated onto a Si wafer at 1300 rpm for 60 s. Before each measurement, the surfaces were annealed at 150 °C in an oven under vacuum overnight. For SFG experiments, 1.5% PS/PAA in THF solution was spin-coated (1300 rpm, 60 s) on the top CaF_2 windows (Ø 25 ± 0.1 mm × 2 ± 0.1 mm) purchased from CRYSTAL GmbH, resulting in a thickness of 130 ± 10 nm as measured with a profilometer (P-7 Stylus Profiler, KLA-Tencor). The resulting samples were annealed at 150 °C for 1 h in an oven before their usage. The aver-

age roughness of the surface after annealing corresponded to ≈0.27 nm. Then, the authors placed a 10 µL water drop on the surface for 30 min and measured afterward the roughness again. They obtained an average value of ≈0.28 nm, which was similar to the value before contact with water (Section S8, Supporting Information).

Static Advancing Contact Angle Measurement: A 10 µL water drop was deposited on the surface after annealing at different temperatures and after contacting with water for 30 min each. Then 20 µL of DI water was pumped into the drop by a Hamilton syringe (100 µL) with a hydrophobic needle. The process was repeated on three different positions of the surfaces. Inflation was imaged using a camera from side view. The advancing contact angles were calculated by fitting an elliptical model to the images recorded.

Sliding Drop Measurement: 33 µL water drops were deposited on 30° tilted 8.7/1 PS/PAA surfaces at intervals of 1 min by a syringe pump (KD Scientific, Legato 100 Syringe Pump). After 1, 10, and 30 h of exposing to air subsequently, 25 drops were deposited at the same position after every exposing to air. To ensure the surface could recover, the surface was finally annealed at 150 °C for 10 min and 25 drops were deposited on the surface again. The sliding drops were recorded after they had slid on the surfaces for 1 cm by a high-speed camera (Photron, FASTCAM MINI UX100, 1000 fps, with 1× SilverTL Telecentric Lens, Edmund Optics). The recorded slide length of the drop was 1 cm. The velocity of every drop was an average velocity of 1 cm sliding. The details regarding calculating the drop velocity, dynamic advancing and receding contact angles from the recorded video can be found in the authors' previous work.[13]

SFG Measurement: The SFG spectra were measured with a setup based on a femtosecond Ti:sapphire amplified laser. (Coherent Libra, ≈800 nm, ≈50 fs, 1 kHz, 5.2 W). The narrowband (full width of half maximum [FWHM], 20 cm^{-1}) VIS beam was produced by passing part of the laser output through a Fabry–Perot etalon. The broadband (FWHM: 260 cm^{-1}) IR beam was generated by pumping an optical parametric amplifier (TOPAS) in combination with a non-collinear difference frequency generator with a part of the laser output. Both beams (IR: 6.5 mW and VIS: 21 mW) were overlapped spatially and temporally at the surface of the sample with angles of $\theta_{IR} \approx 40°$ and $\theta_{VIS} \approx 60°$ with respect to the surface normal. This produced an SFG signal detected by an electron multiplied charge-coupled device camera (Newton EMCCD) after being dispersed in a spectrometer (Andor Shamrock 303i). All spectra reported in the main text were recorded in SSP (s-polarized SFG, s-polarized VIS, and p-polarized IR) polarization combination during 1 min. Spectra for different polarization combinations and in different frequency regions can be found in the Supporting Information.

Sample Wetting during SFG Experiments: The samples were kept in the flow cell mounted into a stage. For wetting the sample, demineralized water (18.2 mΩ cm) was pumped inside the flow cell by means of tubes (Versilon AE30012 3/16″ inner diameter, 5/16″ out diameter) and a manually controlled peristaltic pump (Masterflex L/S Model: 07559-07). The water was introduced with a flow rate of ≈1 mL s^{-1} (laminar flow) until the tube system was filled up. The water was kept in contact with the sample for 3 min and then removed with the same flow rate used for its introduction. After water removal, the tubes were dried under a dry airflow until no water droplets were visualized inside the cell.

SFG Data Processing: An SFG spectrum of a buried gold sample was used to correct the frequency dependence of the authors' IR beam. A background was acquired for all spectra (gold and samples) by measuring with a blocked IR beam. For normalizing the data, every background was subtracted from its corresponding spectrum and the result was divided by the background-corrected gold spectrum. The calibration of the wavelengths was performed by using a PS foil introduced in the IR path during gold signal measurements. The resulting spectrum had dips corresponding to the PS infrared absorption that could be used to calibrate the wavelength.

Supporting Information

Supporting Information is available from the Wiley Online Library or from the author.

Acknowledgements

X.L. and M.E. contributed equally to this work. The authors thank Gunnar Kircher and Jürgen Thiel for synthesizing the PS/PAA copolymer and PS polymer, respectively. The authors acknowledge financial support by the German Research Society (DFG) via the CRC 1194 (Project-ID 265191195) "Interaction between Transport and Wetting Processes", project C07 and the Priority Programme 2171 Dynamic wetting of flexible, adaptive, and switchable surfaces (BA 5008/5-1 and BU 1556/36-1).

Open access funding enabled and organized by Projekt DEAL.

Conflict of Interest

The authors declare no conflict of interest.

Data Availability Statement

The data that support the findings of this study are available from the corresponding author upon reasonable request.

Keywords

adaptation, contact angles, dynamic contact angles, sum frequency generation

Received: November 2, 2021
Revised: February 9, 2022
Published online:

[1] H.-J. Butt, R. Berger, W. Steffen, D. Vollmer, S. A. L. Weber, *Langmuir* **2018**, *34*, 11292.
[2] W. S. Y. Wong, L. Hauer, A. Naga, A. Kaltbeitzel, P. Baumli, R. Berger, M. D'Acunzi, D. Vollmer, H.-J. Butt, *Langmuir* **2020**, *36*, 7236.
[3] R. Zhang, K. Graf, R. Berger, *Appl. Phys. Lett.* **2006**, *89*, 223114.
[4] I. Tokarev, S. Minko, *Soft Matter* **2009**, *5*, 511.
[5] S. Minko, M. Müller, M. Motornov, M. Nitschke, K. Grundke, M. Stamm, *J. Am. Chem. Soc.* **2003**, *125*, 3896.
[6] S. Lee, S. M. Flores, R. Berger, J. S. Gutmann, M. Brehmer, L. Conrad, L. Funk, P. Theato, D. Y. Yoon1, *J. Plast. Film Sheeting* **2015**, *31*, 434.
[7] L. Ionov, S. Minko, *ACS Appl. Mater. Interfaces* **2012**, *4*, 483.
[8] S. Minko, D. Usov, E. Goreshnik, M. Stamm, *Macromol. Rapid Commun.* **2001**, *22*, 206.
[9] J. A. Crowe, J. Genzer, *J. Am. Chem. Soc.* **2005**, *127*, 17610.
[10] G. D. Crevoisier, P. Fabre, J.-M. Corpart, L. Leibler, *Science* **1999**, *285*, 1246.
[11] B. K. Crone, A. Dodabalapur, R. Sarpeshkar, A. Gelperin, H. E. Katz, Z. Bao, *J. Appl. Phys.* **2002**, *91*, 10140.
[12] H. Kuroki, I. Tokarev, S. Minko, *Annu. Rev. Mater. Res.* **2012**, *42*, 343.
[13] X. Li, S. Silge, A. Saal, G. Kircher, K. Koynov, R. Berger, H.-J. Butt, *Langmuir* **2021**, *37*, 1571.
[14] Y. R. Shen, *Nature* **1989**, *337*, 519.
[15] C. Cai, M. S. Azam, D. K. Hore, *J. Phys. Chem. C* **2021**, *125*, 12382.
[16] A. G. Lambert, P. B. Davies, D. J. Neivandt, *Appl. Spectrosc. Rev.* **2005**, *40*, 103.
[17] X. Li, X. Lu, *Macromolecules* **2018**, *51*, 6653.
[18] H. Tsuruta, Y. Fujii, N. Kai, H. Kataoka, T. Ishizone, M. Doi, H. Morita, K. Tanaka, *Macromolecules* **2012**, *45*, 4643.

[19] K. A. Briggman, J. C. Stephenson, W. E. Wallace, L. J. Richter, *J. Phys. Chem. B* **2001**, *105*, 2785.
[20] P. Balzerowski, K. Meister, J. Versluis, H. J. Bakker, *Phys. Chem. Chem. Phys.* **2016**, *18*, 2481.
[21] A. B. D. Cassie, *Discuss. Faraday Soc.* **1948**, *3*, 11.
[22] N. Dhopatkar, E. Anim-Danso, C. Peng, S. Singla, X. Liu, A. Joy, A. Dhinojwala, *Macromolecules* **2018**, *51*, 5114.
[23] A. Horinouchi, H. Atarashi, Y. Fujii, K. Tanaka, *Macromolecules* **2012**, *45*, 4638.
[24] I. Luzinov, S. Minko, V. V. Tsukruk, *Prog. Polym. Sci.* **2004**, *29*, 635.
[25] S. Schubotz, C. Honnigfort, S. Nazari, A. Fery, J.-U. Sommer, P. Uhlmann, B. Braunschweig, G. K. Auernhammer, *Adv. Colloid Interface Sci.* **2021**, *294*, 102442.
[26] S. Santer, A. Kopyshev, J. Donges, H.-K. Yang, J. Rühe, *Langmuir* **2006**, *22*, 4660.
[27] L. Chen, E. Bonaccurso, T. Gambaryan-Roisman, V. Starov, N. Koursari, Y. Zhao, *Curr. Opin. Colloid Interface Sci.* **2018**, *36*, 46.

